

Regiocontrol via Electronics: Insights into a Ru-Catalyzed, Cu-Mediated Site-Selective Alkylation of Isoquinolones via a C–C Bond Activation of Cyclopropanols

Neha Jha,^[a] Wentao Guo,^[b] Wang-Yeuk Kong,^[b] Dean J. Tantillo,^{*,[b]} and Manmohan Kapur^{*,[a]}

A site-selective C(3)/C(4)-alkylation of *N*-pyridylisoquinolones is achieved by employing C–C bond activation of cyclopropanols under Ru(II)-catalyzed/Cu(II)-mediated conditions. The regioisomeric ratios of the products follow directly from the electronic nature of the cyclopropanols and isoquinolones used, with electron-withdrawing groups yielding predominantly the C(3)-alkylated products, whereas the electron-donating groups

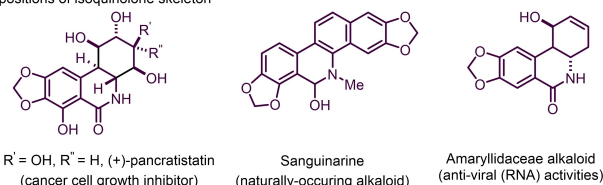
primarily generate the C(4)-alkylated isomers. Density functional theory calculations and detailed mechanistic investigations suggest the simultaneous existence of the singlet and triplet pathways for the C(3)- and C(4)-product formation. Further transformations of the products evolve the utility of the methodology thereby yielding scaffolds of synthetic relevance.

Introduction

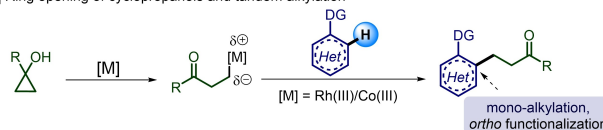
The efficient construction of diversely functionalized heterocycles, particularly isoquinolone derivatives, has long been an attractive target in synthetic chemistry. Owing to their extensive biological activities and prevalence in naturally occurring alkaloids as well as therapeutic agents,^[1] numerous synthetic routes have been designed over the years to achieve this framework (Scheme 1a).^[2] Site-selectivity has invariably been an important theme in C–H functionalization of heteroarenes, and in this regard isoquinolones are no exception. Thus, controlling the same is a crucial challenge, which is often overcome by the introduction of directing groups and upon tuning the catalyst system. In this context, Hong and co-workers described a site-selective C(4)- vs C(8)-arylation of isoquinolones by switching the metal catalyst from [Pd] to [Ir].^[2a] A similar modulation of regioselective C(4)/C(8)-alkynylation of isoquinolones was achieved by Patil and co-workers, utilizing [Au] and [Rh] complexes respectively,^[2b] whilst Samanta and co-workers accomplished a regiocontrolled C(3)/C(8)-amidation of isoquinolones under Ir(III)-catalysis.^[2c]

Site-selective introduction of β -ketoaryl groups to arenes/heteroarenes is gaining significance for promoting late-stage functionalization in numerous contexts. One of the techniques for achieving this goal involves ring opening of strained, small-

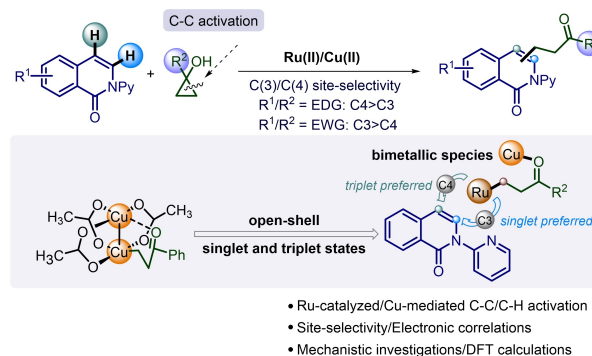
a | Important drug molecules and natural products bearing substituents at the C(3)/C(4) positions of isoquinolone skeleton



b | Ring opening of cyclopropanols and tandem alkylation⁷



c | Present Approach: Influence of electronic environment of cyclopropanols and isoquinolones on selective C(3)/C(4)-alkylation



Scheme 1. Backdrop and synopsis of the present work.

ring systems.^[3] In this regard, cyclopropanols act as one of the best suited substrates owing to their facile syntheses and propensity to form homoenolates/ β -ketoalkyl radicals under transition metal (TM)-catalyzed conditions, thereby acting as nucleophiles or electrophiles respectively.^[4] Such disconnections of C–C bonds promoted by TM-catalysis can either be via oxidative insertion of the TM into the C–C bond or β -C elimination, thus assisting in facile C–C bond formation.^[5]

[a] N. Jha, Prof. M. Kapur
Department of Chemistry
Indian Institute of Science Education and Research Bhopal
Bhopal 462066, MP (India)
E-mail: mk@iiserb.ac.in

[b] W. Guo, W.-Y. Kong, Prof. D. J. Tantillo
Department of Chemistry
University of California–Davis
Davis, California 95616 (USA)
E-mail: djtantillo@ucdavis.edu

Supporting information for this article is available on the WWW under <https://doi.org/10.1002/chem.202301551>

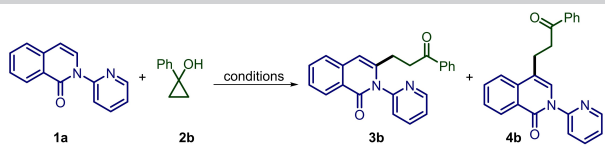
Hence, methods emerging from the combination of both, the C–H and C–C bond activation strategies, are desirable for effective construction of alkylated heteroarenes (Scheme 1b).^[6] Towards this, Li and co-workers reported a Rh(III)-catalyzed *ortho* C–H alkylation of arenes via concomitant ring opening of cyclopropanols, driven primarily by chelation assistance strategy.^[7(a),(b)] Moreover, Liu and co-workers had elaborated upon the oxidative cyclization of oxazolines resulting from a similar ring cleavage protocol.^[7(c)] Recently, Anbarasan and co-workers described a C(2)-alkylation of indoles under Rh- and Co-catalysis.^[7(d),(e)]

Given the utility and prevalence of functionalized isoquinolines and isoquinolones, we have been investigating methods for their site-selective C(3)/C(4)-functionalization.^[8] For this purpose, we thought of utilizing cyclopropanols as the active congeners since they are known to generate β -functionalized ketone motifs. During our efforts to design an appropriate methodology, we discovered that the propensity of cyclopropanols to couple with the C(3)- or C(4)-positions of isoquinolones was dependent entirely upon the electronic environment around the three-membered ring as well as it relied upon the transition metal catalyst used. In this work, we report a Ru-catalyzed, Cu-mediated, site-selective C(3)/C(4)-alkylation of *N*-pyridyl isoquinolones resulting from the concomitant C–H and C–C bond activation approaches (Scheme 1c). In our studies, we realized the involvement of either of the transition metals in the cyclopropanol ring cleavage that form reactive intermediates for facile C(3)/C(4)-H functionalization. The same transformation, when performed in the presence of [Cp*RhCl₂]₂, led to an exclusive formation of the C(3)-isomer, regardless of the electronic variations. This anomaly in the site-selectivity was rationalized through a series of control experiments, mechanistic investigations and DFT calculations.

Results and Discussions

To explore the feasibility of our approach, we initiated our investigations by using 2-(pyridin-2-yl)isoquinolin-1(2*H*)-one (**1a**) and 1-phenylcyclopropan-1-ol (**2b**) as the model substrates for optimization (Table 1). We initiated our screening by employing [Cp*RhCl₂]₂ as the catalyst, along with CsOAc and Cu(OAc)₂·H₂O as the additive and oxidant respectively, in MeOH as the solvent (entry 1, Table 1). The C(3)-coupled product was formed exclusively with no trace of the C(4)-isomer. To achieve our goal of obtaining site-selectivity, we next screened the various transition metal catalysts (entries 2, 4 and 5, Table 1), out of which the Ru-catalyst offered the desired result with an initial yield of 20% and a 3:1 ratio of the C(3):C(4)-alkylated products. The effect of the reaction temperature also proved to be a vital parameter, with an improved yield obtained at 80 °C (entries 2 and 3, Table 1). Next, the role of different additives in the reaction outcome was examined. The replacement of CsOAc with Ag(I) salts did not result in a significant increment in yields (entries 6 and 7, Table 1). Addition of 1-AdCO₂H, in turn, afforded the best result with an overall isolated yield of 73%, whereas other carboxylic acid

Table 1. Optimization of the reaction conditions.^[a,c]



Entry	Catalyst/Additive/Oxidant	Solvent	Temp [°C]	Yield [%] ^[b]
1 ^c	[Cp*RhCl ₂] ₂ /CsOAc/Cu(OAc) ₂ ·H ₂ O	MeOH	RT	65
2	[Ru(<i>p</i> -cym)Cl ₂] ₂ /CsOAc/Cu(OAc) ₂ ·H ₂ O	MeOH	RT	20
3	[Ru(<i>p</i> -cym)Cl ₂] ₂ /CsOAc/Cu(OAc) ₂ ·H ₂ O	MeOH	80	45
4	Pd(OAc) ₂ /CsOAc/Cu(OAc) ₂ ·H ₂ O	MeOH	80	NR
5	[Cp*IrCl ₂] ₂ /CsOAc/Cu(OAc) ₂ ·H ₂ O	MeOH	80	NR
6	[Ru(<i>p</i> -cym)Cl ₂] ₂ /AgSbF ₆ /Cu(OAc) ₂ ·H ₂ O	MeOH	80	16
7	[Ru(<i>p</i> -cym)Cl ₂] ₂ /AgBF ₄ /Cu(OAc) ₂ ·H ₂ O	MeOH	80	48
8	[Ru(<i>p</i> -cym)Cl ₂] ₂ /PivOH/Cu(OAc) ₂ ·H ₂ O	MeOH	80	45
9	[Ru(<i>p</i> -cym)Cl ₂] ₂ /1-AdCO ₂ H/Cu(OAc) ₂ ·H ₂ O	MeOH	80	73
10	[Ru(<i>p</i> -cym)Cl ₂] ₂ /PhCO ₂ H/Cu(OAc) ₂ ·H ₂ O	MeOH	80	47
11	[Ru(<i>p</i> -cym)Cl ₂] ₂ /1-AdCO ₂ H/Cu(OAc) ₂ ·H ₂ O	EtOH	80	48
12 ^[d]	[Ru(<i>p</i> -cym)Cl ₂] ₂ /1-AdCO ₂ H/Cu(OAc) ₂ ·H ₂ O	TFE	80	42
13 ^[e]	[Ru(<i>p</i> -cym)Cl ₂] ₂ /1-AdCO ₂ H/Cu(OAc) ₂ ·H ₂ O	HFIP	80	45

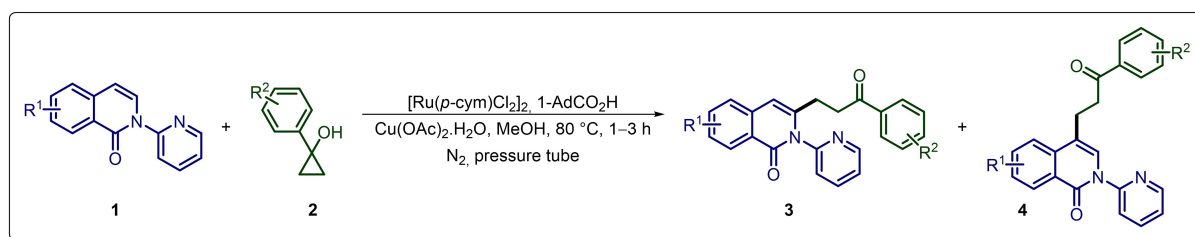
[a] Unless otherwise mentioned, all reactions were carried out using **1a** (0.1 mmol, 1.0 equiv.), **2b** (0.2 mmol, 2.0 equiv.), catalyst (4 mol%), additive (25 mol%), oxidant (2.1 equiv.) in solvent (1 mL) for 3 h in a pressure tube. [b] Isolated yields. [c] Relative ratio of C(3):C(4) isomer = 3:1 deduced via ¹H NMR analysis of the crude reaction mixture. [d] C(3):C(4) = 4.5:1. [e] C(3)-isomer exclusively. NR = No Reaction.

additives did not yield notable results (entries 8–10, Table 1). Polar protic solvents were the best choices for the transformation, where MeOH proved to be the most suitable amongst those scanned. It must be noted here that the ratio of the C(3):C(4) coupled products did not vary significantly for reactions carried out in MeOH or EtOH, but a predominant solvent effect was observed upon increasing the polarity. Fluorinated alcoholic solvents such as TFE yielded the C(3)-alkylated product predominantly (C(3):C(4) = 4.5:1), whereas HFIP resulted in the formation of the C(3) isomer exclusively (entries 11–13, Table 1).^[9]

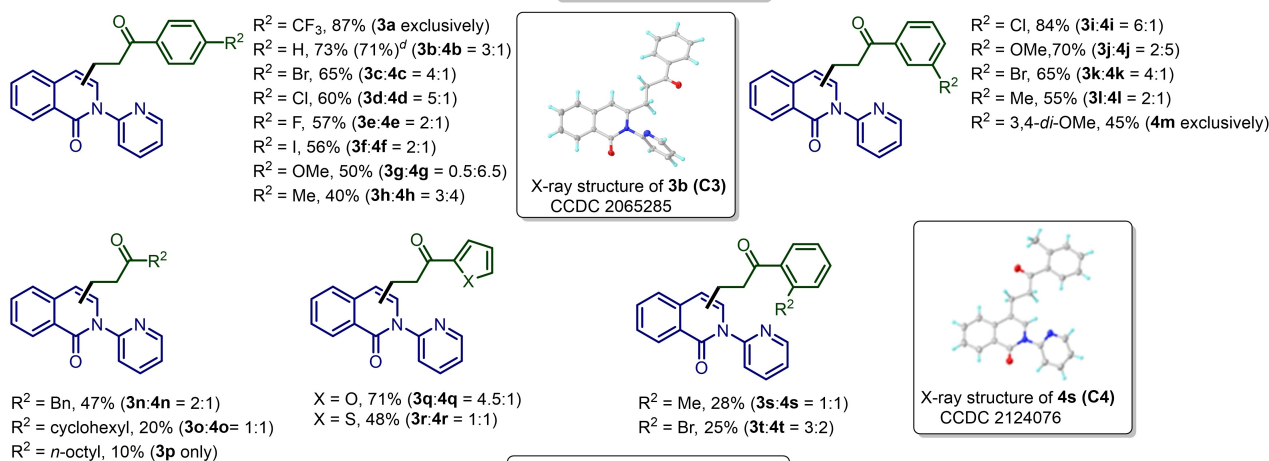
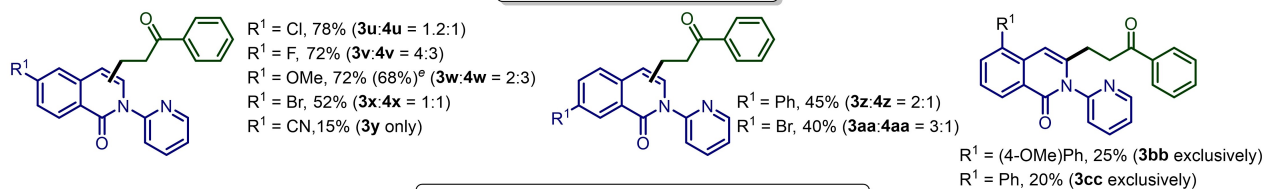
With the optimized condition in hand, we then began screening various substrates for compatibility with the transformation. Interestingly, it was observed that the electronic environment of the substituents on the aryl ring of the cyclopropanol largely dictated the product regioselectivity. For instance, a preferential alkylation at the C(3)-position was

obtained when EWG groups such as $-\text{CF}_3$ was present *para* to the quaternary ring carbon (**3a**, Scheme 2). However, if a strong EDG such as *p*-OMe was present, C(4)-coupled product was obtained as the major isomer (**3g/4g**, Scheme 2). Specifically,

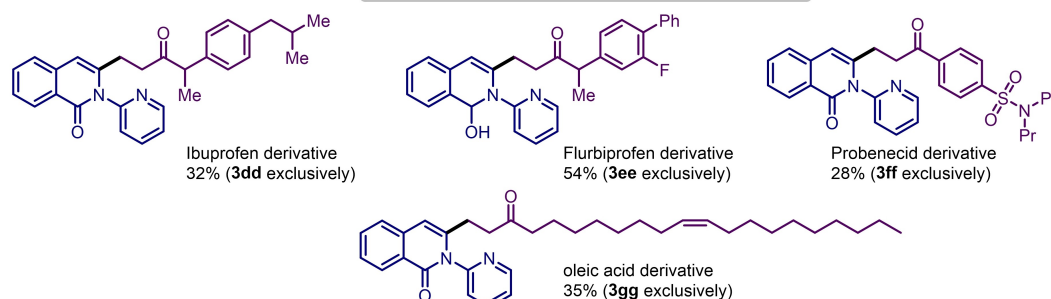
we obtained products representing the two extremities of selectivity, *i.e.*, *p*- CF_3 and 3,4-*di*-OMe, affording the C(3)- and C(4)-isomers exclusively (**3a**, **4m**, Scheme 2). Substituents whose electronic nature lay between these two extremities



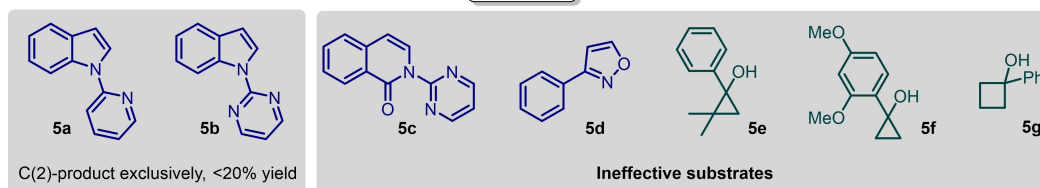
Scope of cyclopropanols

Scope of *N*-pyridylisoquinolones

Late stage modification of drugs and natural products



Limitations



Scheme 2. Substrate scope for site-selective C(3)/C(4)-alkylation.^[a,b,c] [a] Reaction conditions: **1** (0.1 mmol), **2** (0.2 mmol), $[\text{Ru}(p\text{-cym})\text{Cl}_2]_2$ (4 mol%), 1-AdCO₂H (25 mol%), $\text{Cu}(\text{OAc})_2 \cdot \text{H}_2\text{O}$ (2.1 equiv) in 1 mL of MeOH at 80 °C in a pressure tube. [b] Isolated yields after column chromatography. [c] Relative ratio of the C(3):C(4) are calculated through crude ¹H NMR. [d] Performed on a 1 mmol scale; combined yield of **3b/4b**: 71%. [e] Yield of gram scale reaction.

yielded a mixture of the two isomers in a ratio determined solely by their electronic push/pull effects (**3b/4b–3h/4h**, Scheme 2).

For *meta* substituted arenes, a similar trend was observed; *m*-Cl revealed a greater inclination towards C(3)-alkylation as compared to *m*-Me (**3i/4i**, **3l/4l**, Scheme 2). Complementary observation was detected for *m*-OMe and *m*-Br as well, considering their inductive effects (**3j/4j** and **3k/4k**, Scheme 2). The feasibility of the transformation was extended to aliphatic cycloalkanols containing benzyl, cyclohexyl and octyl groups as well, yielding the desired products, *albeit* in lower yields (**3n/4n–3p**, Scheme 2). Poor selectivity was observed in these cases owing to reduced effects of substituent electronics. 1-heteroarylcyclopropanols were also suitable substrates for the transformation with an improved ratio of C(3)/C(4)-products, obtained upon moving from the more electron-withdrawing 2-furyl to comparatively lesser 2-thienyl group (**3q/4q** and **3r/4r**, Scheme 2). In addition to the electronic parameters, steric hindrance also played a vital role, since a decrease in yield arising from both incomplete consumption of the isoquinolone and degradation of the cyclopropanol was observed upon substituting the phenyl group at the *ortho* position (**3s/4s** and **3t/4t**, Scheme 2). 2-alkyl substituted as well as the *o/p*-disubstituted aryl cyclopropanols failed to generate the desired products, probably owing to these steric effects (**5e** and **5f**, Scheme 2). Similar trends were observed upon substituting the 2-(pyridin-2-yl)isoquinolin-1(2*H*)-ones. Substitutions at the 6- and 7-positions of the isoquinolones were well-tolerated, thereby dictating the ratio of the regioisomeric products in accordance with their electronic properties (**3u/4u–3aa/4aa**, Scheme 2). The 6-CN substituent led to a substantial depletion of electron density on the isoquinolone ring and thus generated the C(3)-product exclusively, again in accordance with the traits observed for cyclopropanols (**3y**, Scheme 2). Also, a much-reduced yield was obtained primarily due to the lower solubility of 6-CN substrate in MeOH. For the 5-substituted 2-(pyridin-2-yl)isoquinolin-1(2*H*)-ones, only the C(3)-products were obtained predominantly due to steric congestion faced at the *peri* C(5)-position (**3bb** and **3cc**, Scheme 2). Additionally, as depicted in Scheme 2, decreased product yields were observed for reactions which employed alcohols with EDGs on the phenyl rings as coupling partners. For EWG-containing cyclopropanols, the reaction proceeded to completion with the cycloalkanol persisting in the reaction medium for prolonged period whereas with electron-donating substituents, the isoquinolones were often recovered back. This arises mainly due to their higher oxidation propensity, via ring opening under the reaction conditions.

Late-stage modification of drug molecules and naturally occurring products enhanced the utility of the transformation, thereby providing a scope for their step-economic functionalization (**3dd–3gg**, Scheme 2).

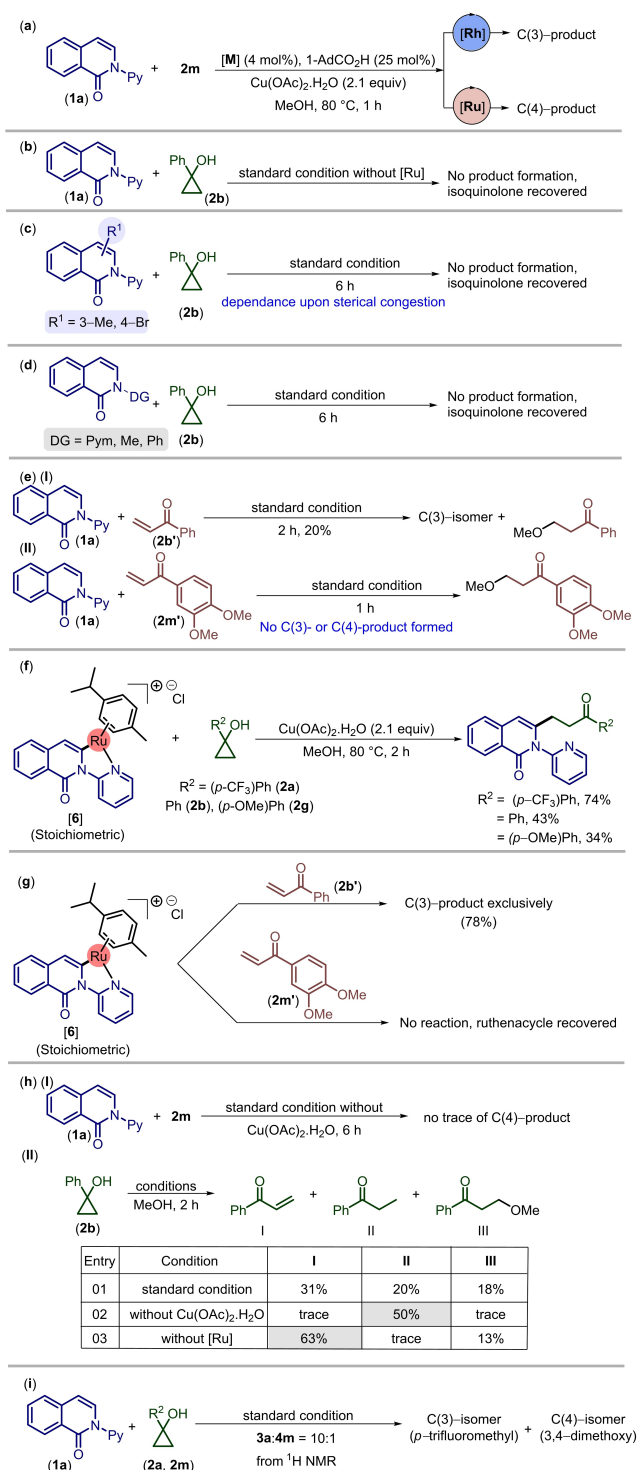
To further validate the site-selective alkylation, a set of *N*-heterocycles known to induce site-selectivity were screened. In this regard, substrates such as 1-(pyridin-2-yl)-1*H*-indole (**5a**, Scheme 2) and 1-(pyrimidin-2-yl)-1*H*-indole (**5b**, Scheme 2), upon subjecting to our optimized reaction condition, resulted

in the C(2)-coupled product formation exclusively, in lower yields, whereas the 3-phenylisoxazole (**5d**, Scheme 2) failed to react. Upon replacing the pyridyl with a pyrimidyl group (**5c**, Scheme 2), no product formation, either at the C(3)- or C(4)-position resulted, thereby indicating that pyridyl is the optimal directing group for the transformation. An attempt to extrapolate the reactivity of cyclopropanols to cyclobutanols did not yield any product (**5g**, Scheme 2).

Mechanistic studies and control experiments

Considering literature reports, we initially proposed two distinctly different pathways for the C(3) and C(4)-alkylation; *i.e.*, pyridyl directed proximal C–H metalation vs. a distal C–H metalation, for C(3)- and C(4)-H activations respectively, in a one-pot fashion.^[6] Given the site-selectivity obtained, which was dependent upon the electronic environment of the coupling partners, as well as to explore the role of each of the reaction components, control experiments were carried out. While both Rh- and Ru-catalysts worked well for the transformation, only the latter demonstrated the regiodivergent selectivity. When 1-(3,4-*di*-methoxyphenyl)cyclopropan-1-ol (**2m**) was used as the coupling partner under Rh-catalyzed condition, exclusive formation of the C(3)-isomer was obtained which remained in contrast to the Ru-catalyzed condition (Scheme 3a, see Scheme S12 of the Supporting Information (SI) for details). No product formation was observed in the absence of the Ru-catalyst which indicated that the catalyst was mandatory for the transformation (Scheme 3b).

Further, to rule out the possibility of a 1,2-migration of the metal either from C(3)- to C(4)- or *vice versa*, either position was blocked. No alkylation was observed, suggesting that the steric hindrance played a pivotal role in the reaction outcome as well as negated the possibility of any migration (Scheme 3c). Also, to rationalize the importance of pyridyl as the optimum directing group, it was replaced with –Me, –Pym and –Ph groups. No alkylation either at the C(3)- or C(4)- was observed, which indicated the importance of the directing group for carrying out the C–H functionalization (Scheme 3d). Further, the detection of trace amounts of enone (**2b'**) in the ¹H NMR of the crude reaction aliquot suggested the involvement of a β-H elimination step, following ring-opening of cyclopropanols.^[7a] Therefore, to probe its participation as an intermediate, 1-phenylprop-2-en-1-one (**2b'**) was independently synthesized and coupled with 2-(pyridin-2-yl)isoquinolin-1(2*H*)-one (**1a**) under the optimized reaction condition. Formation of the alkylated C(3)-product, although with reduced yields, indicated the intermediacy of the enone in one of the steps for C(3)-alkylation pathway (Scheme 3e(i)). No C(4)-product was detected. However, a coupling reaction with 1-(3,4-dimethoxyphenyl)cyclopropan-1-ol (**2m**) (which gave exclusively the C(4)-isomer under standard reaction conditions), when arrested after 2 min, showed significant formation of the corresponding enone (see the Supporting Information (Figure 3) for details). Analogously, a reaction when replicated with 1-(3,4-dimethoxyphenyl)prop-2-en-1-one (**2m'**), showed no trace of either the C(3)- or C(4)-isomer which



Scheme 3. Control experiments.

indicated that the electronically rich enones may not be reactive intermediates in the C(3)-alkylation pathway (Scheme 3e(II)).

Isolation of the five-membered ruthenacycle [6] was crucial for gaining further insight into the reaction pathway. The metalacycle when reacted stoichiometrically with the cyclopropanols (**2a**, **2b**, **2g**) in presence of Cu(OAc)₂·H₂O, yielded

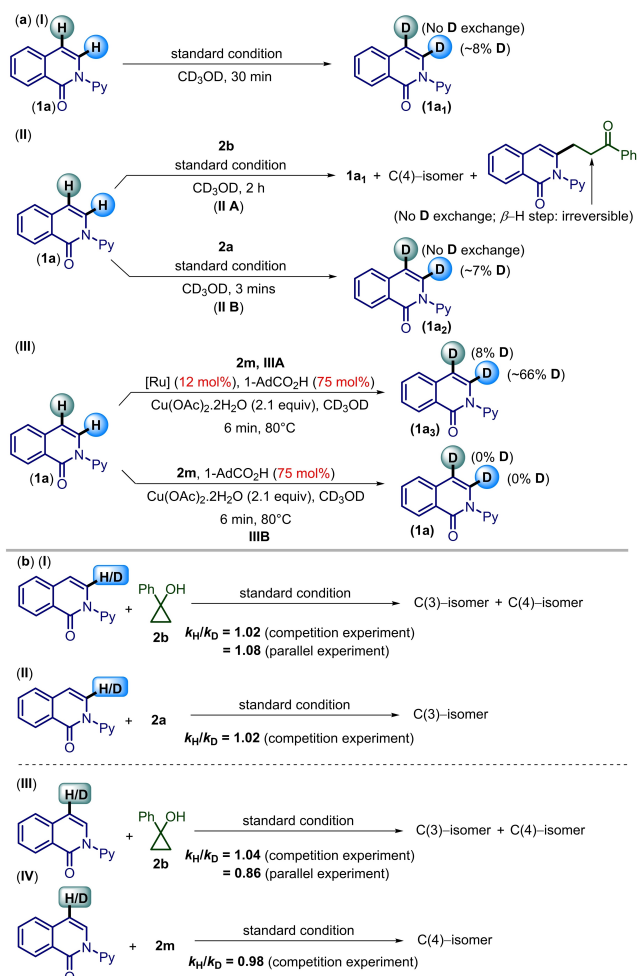
the C(3)-isomer solely, for both electronically neutral and electronically rich alcohols, thereby pointing towards a distinct Ru-catalyzed pathway for the C(4)-alkylation (Scheme 3f). It must be highlighted that electronically deficient alcohols gave better yields as compared to the electronically rich systems, thereby indicating the metalacycle's compatibility with the different cycloalkanols. Also, when a similar reaction was performed by substituting alcohols with enones as the coupling partner, exclusive formation of the C(3)-product occurred for **2b'** whereas **2m'** remained unreacted, thereby further supporting the consistency of the metalacycle with the coupling congeners (alcohols/in situ generated enones) (Scheme 3g).

We next probed the role of Cu(OAc)₂·H₂O in the plausible reaction mechanisms. In addition to acting as an oxidant for the C(3)-alkylation pathway,^[7a] it also contributed towards the ring opening of cyclopropanols,^[10] and was found to be essential for the C(4)-product formation. To further rationalize its role, the reaction involving 1-(3,4-dimethoxyphenyl) cyclopropan-1-ol (**2m**) as the coupling partner, under standard reaction conditions, was performed in the absence of Cu(OAc)₂·H₂O (Scheme 3h(I)). No C(4)-product was observed even after prolonged reaction times. A control reaction when carried out with 1-phenylcyclopropan-1-ol (**2b**) as the substrate, in absence of the Ru-catalyst (entry 3, Scheme 3h(II)), yielded the corresponding enone as the major product. This substantiated the role of Cu(OAc)₂·H₂O in generating the active enone intermediate for the C(3)-alkylation.

Additionally, to probe for the relative rates of alkylation for the electron-donating and electron-withdrawing alcohols, a 1:1 mixture of 1-(4-(trifluoromethyl)phenyl)cyclopropan-1-ol (**2a**) and 1-(3,4-dimethoxyphenyl)cyclopropan-1-ol (**2m**) was taken in the same vessel and subjected to the standard reaction condition. A 10:1 mixture of the respective products was detected (via ¹H NMR) with 1-(4-(trifluoromethyl)phenyl)cyclopropan-1-ol (**2a**) and 2-(pyridin-2-yl)isoquinolin-1(2H)-one (**1a**) persisting in the reaction mixture. This observation also demonstrated the rapid consumption of EDG containing alcohols in the given reaction condition, and hence the observed ratio of products (Scheme 3i). A similar conclusion was drawn through a parallel experiment, run in presence of an internal standard via ¹H NMR experiments (see the Supporting Information (section IX) for details).

Studies to check for the reversibility of the initially proposed C–H activation steps were carried out, both in the presence and absence of the cyclopropanol (Scheme 4a). Initially, deuterium exchange was observed only at the C(3)-position, with no deuteration at the C(4) (Scheme 4a(I)). The experiment when repeated in the presence of EWG-containing alcohol **2a**, yielded a similar conclusion (Scheme 4a(II)). These experiments, in addition to the isolated ruthenacycle, confirm the C(3)-H bond activation.

We next proceeded to probe for the existence of the proposed C(4)-H activation as an intermediate step for the C(4)-alkylation pathway. To check for its reversibility, the reaction was subjected to a higher loading of the ruthenium catalyst and 1-(3,4-dimethoxyphenyl)cyclopropan-1-ol (**2m**) was used as the coupling partner (Scheme 4a(III)). Here too, an 8% D-



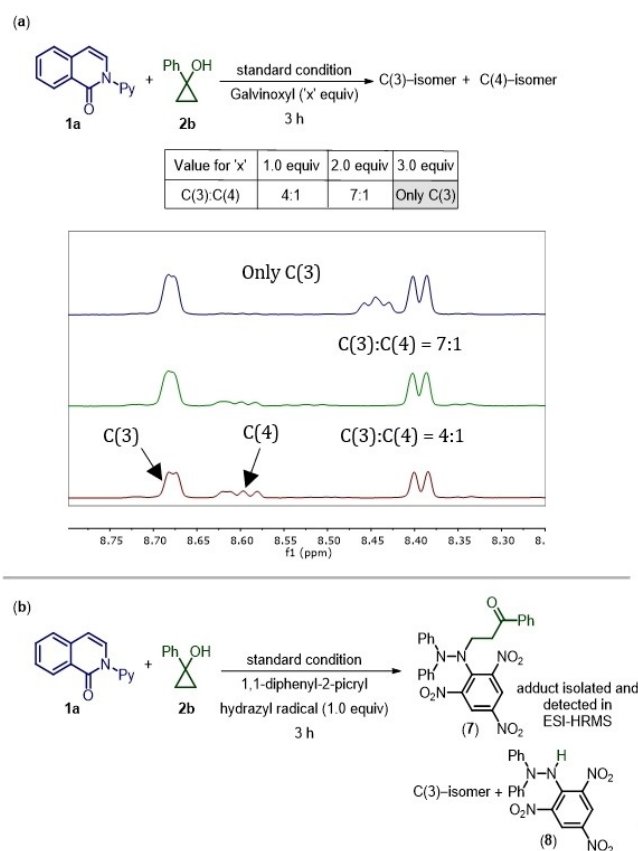
Scheme 4. Mechanistic studies.

incorporation was observed at the C(4). Further, to rule out the possibility of an electrophilic deuteration (via S_EAr), a control reaction was conducted in the absence of [Ru] (Scheme 4a(IIIB)), where no 'H/D' exchange was observed. These results although indicative of a C(4)-H activation, did not yield confirmatory conclusions, unlike C(3). Also, for the C(3)-H activation, no deuterium scrambling occurred at the α -C of the product, suggesting the probable β -H elimination step to be irreversible (Scheme 4a(IIA)). Further, studies to check for a primary kinetic isotope effect in the C(3)-H activation and the probable C(4)-H activation steps were carried out, both via parallel and competition experiments. In either case, no primary KIE was observed which indicated that the turnover limiting step did not involve C–H bond scission (Scheme 4b). In fact, a diminished value of 0.86 for C(4) is indicative of an inverse secondary kinetic isotope effect arising due to a hybridization change at the C(4).^[11] Additionally, competition experiments were performed for EWG and EDG-containing alcohols, thereby attaining similar conclusions (Scheme 4b (II) and (IV)).

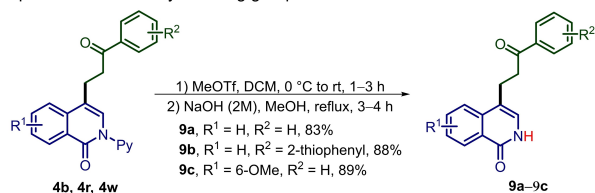
Next, to gain further insights into the mechanism for the C(4)-product formation, a set of experiments were performed where radical scavengers such as TEMPO, BHT, diphenyl

ethylene and galvinoxyl were added into the reaction mixture (Scheme 5). While TEMPO, BHT and diphenylethylene failed to provide conclusive results at the elevated reaction temperature, it was observed that in the case of galvinoxyl, on subsequent increase in the number of equivalents of galvinoxyl used (from 1.0 equiv to 3.0 equiv), a considerable decline in the ratio of the C(3):C(4) isomers was observed (Scheme 5a). This outcome hints towards the probable involvement of a radical pathway for the C(4)-alkylation process and not a C(4)-H activation. Additionally, our findings were further corroborated when an *N*-centered radical quencher such as 1,1-diphenyl-2-picrylhydrazyl yielded the alcohol adduct, with no trace of the C(4)-isomer (Scheme 5b). The fact that **7** did not arise from a conjugate addition of the reagent to the corresponding enone, supported the conclusion that the adduct **7** arose from the quenching of the corresponding β -ketoalkyl radical generated in situ (see the Supporting Information (Scheme S27C) for details).

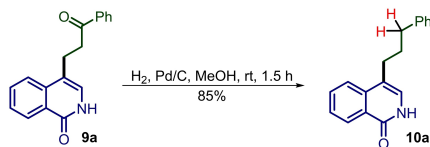
To further enhance the synthetic utility of the alkylated products, the pyridyl directing group was deprotected. Here, the C(4)-alkylated isomers gave exclusively the corresponding *N*-deprotected isoquinolones in appreciable yields (**9a–9c**, Scheme 6(i)). Also, an access to propyl substituted isoquinolones was achieved, upon subjecting the C(4)-*N*-deprotected isomer to hydrogenolysis (**10a**, Scheme 6(ii)). Such propyl substituted isoquinolone scaffolds are difficult to synthesize via

Scheme 5. Effect of galvinoxyl: ¹H NMR plot showing its diminishing effect on the C(4)-isomer formation; adduct formation with 1,1-diphenyl-2-picrylhydrazyl radical.

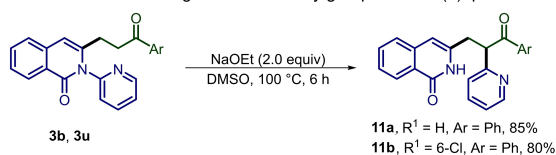
(i) Deprotection of the –Py directing group.



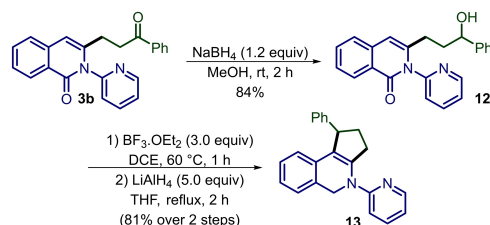
(ii) Synthesis of C(4)–propyl substituted isoquinolones.



(iii) Tandem removal and rearrangement of the –Py group for the C(3)–product.



(iv) Intramolecular electrophilic cyclization: Formation of 6,6,5-fused isoquinolone scaffolds.



Scheme 6. Synthetic transformations.

conventional methods and hence, the present approach assists in assembling the same step-economically.

Also, in continuation with our efforts to obtain the pyridyl group deprotection for the C(3)-isomer, a concomitant removal and rearrangement of the directing group was observed (**11a–11b**, Scheme 6(iii)). Simultaneously, we were also successful in constructing a 6,6,5-tricyclic scaffold **13**, which finds widespread prevalence in many natural products.^[12] The reaction proceeds through an intramolecular electrophilic cyclization of the corresponding alcohol **12** at the C(4) and subsequent amide reduction.

Computational investigations

To further understand the overall reaction mechanism and the energetics governing the C(3)- and C(4)-alkylation selectivity, we performed Density Functional Theory (DFT) computations at the PBE0-D4/def2-TZVPP//SMD(MeOH)-PBE0-D3(BJ)/def2-SVP level of theory using Gaussian16 and ORCA (see the Supporting Information for computational details).^[13] Conformational searching was carried out using the conformer-rotamer ensemble search tool (CREST) with the GFN2-xTB method.^[14] Wavefunction stability was verified for all singlet structures. Both

singlet and triplet states were considered throughout (see the Supporting Information for preliminary studies on quintet state structures, which were found to be energetically irrelevant for the pathways presented here). Various metal-ligand combinations were considered (see the Supporting Information for details), but only the most energetically favorable are discussed below.

We began by modeling the cyclopropanol ring-opening with $\text{Cu}_2(\text{OAc})_4(\text{MeOH})_2$ as shown in Figure 1. A concerted deprotonation/ring-opening is predicted to form the organocuprate intermediate **IN** via **TSA**. The deprotonation is facilitated by the acetate ligand on one copper, while the homoenolate formed following the ring-opening is coordinated to the other copper atom. This process is predicted to proceed with a reasonable barrier of 24 kcal/mol on both singlet and triplet surfaces. Enone formation is enabled via deprotonation mediated by an acetate ligand and tandem Cu oxidation ($\Delta G^\ddagger = 27$ and 28 kcal/mol on triplet and singlet surface, respectively).

We arrived at two distinct mechanisms for the C(3)- and C(4)-alkylation (Figure 2). For the C(3)-alkylation, we predict a C(3)-H activation via concerted metalation deprotonation (CMD) through **TS1_{C3}**, which generates the five-membered metalacycle **IM1_{C3}**, following dissociation of the acetic acid ($\Delta G^\ddagger = 25$ kcal/mol on the singlet surface).

Further oxidative transmetalation, in which the alkyl group is transferred from the organocuprate **IN** and the *p*-cym ligand dissociates, yields **IM2_{C3}**. Finally, reductive coupling via **TS2_{C3}** ($\Delta G^\ddagger = 26$ kcal/mol on the triplet surface, rate determining for the C(3)-pathway) leads to the formation of the C(3)-activation

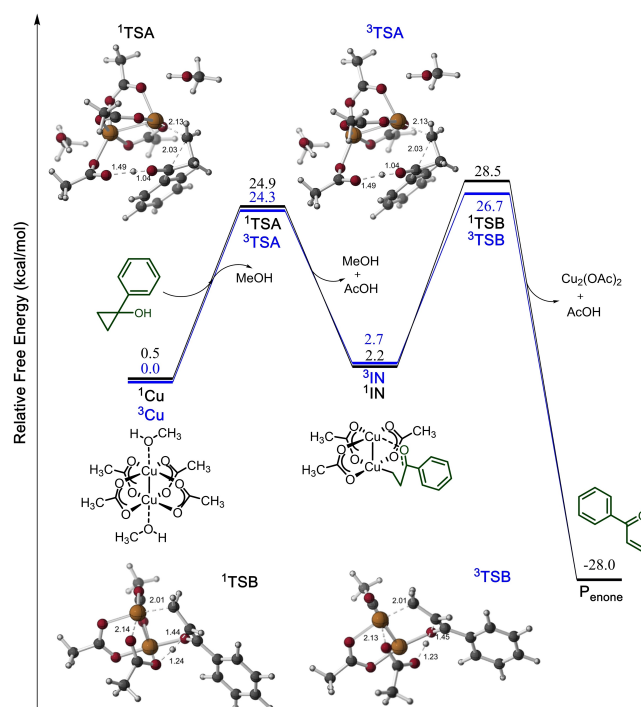


Figure 1. Computed free-energy profile of Cu-mediated ring opening of **2b** in kcal/mol at PBE0-D4/def2-TZVPP//SMD(MeOH)-PBE0-D3(BJ)/def2-SVP level of theory. Selected distances are shown in Å.

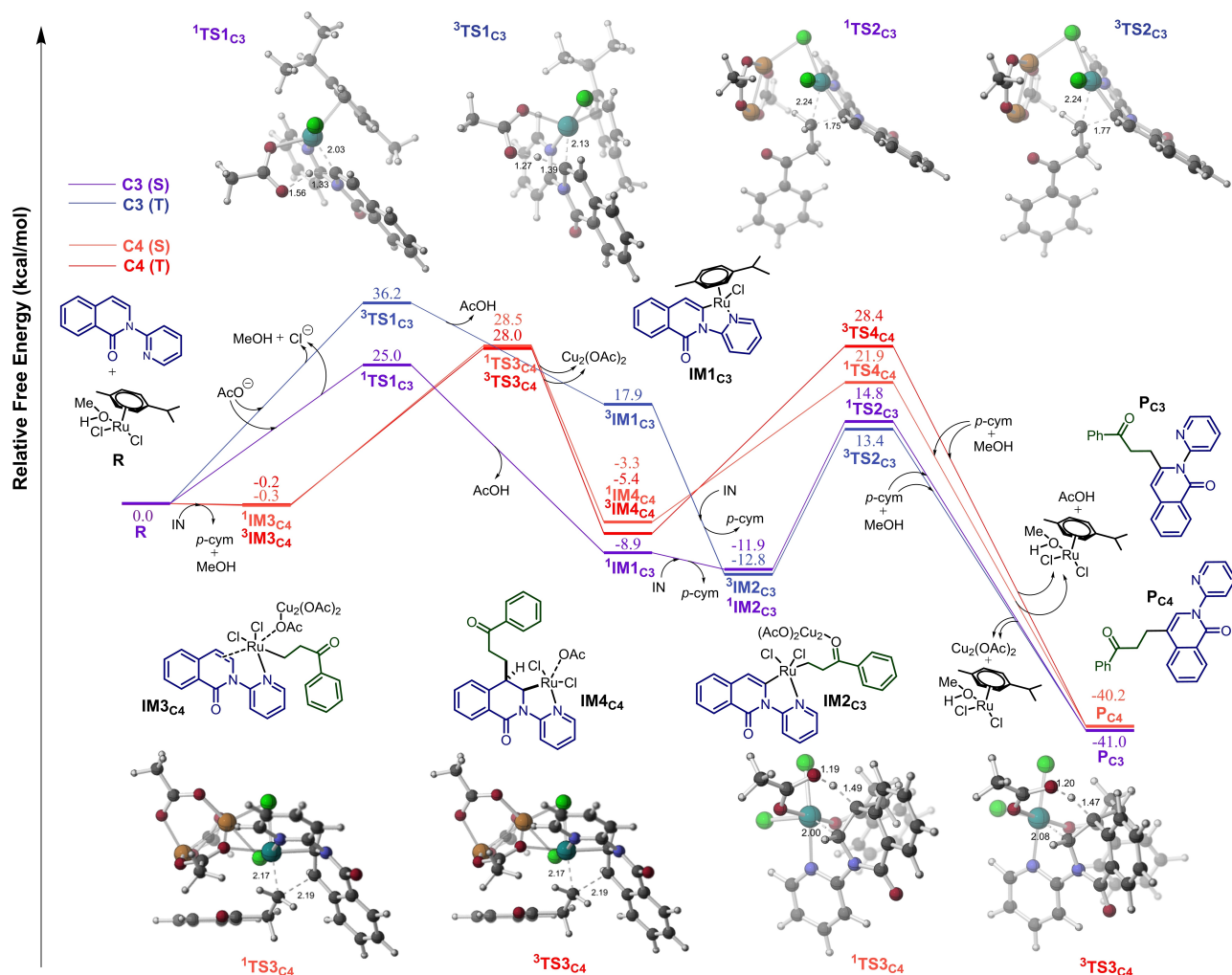


Figure 2. Free-energy profile of **3b** and **4b** generation in kcal/mol at PBE0-D4/def2-TZVPP//SMD(MeOH)-PBE0-D3(BJ)/def2-SVP level of theory. Selected distances are shown in Å.

product **P_{C3}**. We excluded other mechanism that proceed without a CMD step due to high predicted activation barriers (see the Supporting Information for details).

In contrast, we predict that the C(4)-alkylation proceeds through a distinctly different mechanism. Following transmetalation from **IN**, dissociation of the *p*-cym ligand and association of the isoquinolone substrate forms **IM_{3C4}**. A 1,3-alkyl migration then leads to intermediate **IM_{4C4}** through **TS_{3C4}** ($\Delta G^\ddagger = 28$ kcal/mol on the triplet surface). Facile intramolecular deprotonation by an acetate ligand (**TS_{4C4}**, $\Delta G^\ddagger = 22$ kcal/mol on the singlet surface) leads to the C(4)-alkylation product. This mechanism is predicted to prevail over any C(4) CMD C–H activation process for which barriers of at least 31 kcal/mol are predicted (see the Supporting Information for details). Significant diradicaloid character at **TS_{3C4}** and **TS_{4C4}** is consistent with inhibition by radical scavengers (see the Supporting Information for spin population analysis).

To account for the formation of the C(3)-product when reacting the enone and **IM_{1C3}** in the absence of $\text{Cu}_2(\text{OAc})_4$, we computed the reaction as shown in Figure 2 (see also Scheme 3(g)). The computed coupling step via migratory

insertion of the enone to the $\text{C}(sp^2)\text{--Ru}$ bond is predicted to have a reasonable barrier of 23 kcal/mol on the singlet surface, leading to **IM_{6C3}**. Protodemetalation with acetic acid ensues ($\Delta G^\ddagger = 2.3$ kcal/mol), forming the C(3)-product. Under the standard reaction conditions used, **IM_{1C3}** can, in principle, react with either **IN** or enone generated in situ by cyclopropanol and Cu. However, the formation of enone requires the cyclopropanol to overcome a 27 kcal/mol barrier through **TS_B**, which is higher than the (now rate-determining) coupling barrier via **TS_{2C3}**. Interestingly, neither pathway is kinetically controlled by the initial CMD step ($\Delta G^\ddagger = 25$ kcal/mol). The existence of the two mechanisms for the C(3)-product formation is consistent with the experimental result in Scheme 5(a). The fact that the formation of the C(3)-product cannot be deterred by the radical scavengers also indicates that the C(3)-enone coupling pathway lacks intermediates with radical character.

While the selectivity of the reaction is not perfectly reproduced, $\Delta\Delta G^\ddagger = 3$ kcal/mol of the C(3) compared to C(4) pathway is within error for DFT calculations and accounts for formation of both products. These mechanisms are also consistent with the results of the KIE experiments. For the C(3)

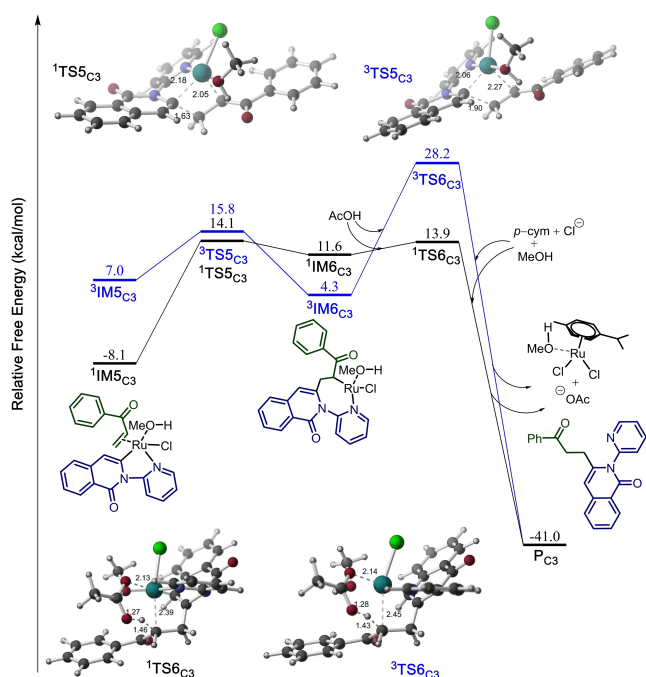


Figure 3. Computed free-energy profile of enone coupling mechanism for C3 at PBE0-D4/def2-TZVPP//SMD(MeOH)-PBE0-D3(BJ)/def2-SVP level of theory. Selected distances are shown in Å.

pathway, these experiments suggested that the CMD step is not rate-determining. For C(4), an inverse secondary KIE was observed, consistent with the DFT prediction that $TS3_{C4}$, with a $Csp^2 \rightarrow Csp^3$ hybridization change, is rate-determining.

Based on the above experimental investigations and Density Functional Theory calculations, a plausible mechanism is proposed in Scheme 7. Two distinctly different catalytic pathways are suggested to operate simultaneously, with the initial step involving ligand exchange of the dimer with MeOH to form the [Ru] species I. For the C(3)-catalytic cycle, three pathways are proposed to be operative. After an initial C(3)-H activation assisted by the acetate or adamantane carboxylate and the pyridyl groups, a five membered ruthenacycle $IM1_{C3}$ is generated; the intermediate being confirmed by spectroscopic analysis (see the Supporting Information (Scheme S16) for details). The pathway **A** involves an oxidative transmetalation,^[15] in which the alkyl group from the Cu-homoenolate species **IN** gets transferred to $IM1_{C3}$ and a ligand exchange with *p*-cym generates the intermediate bimetallic complex $IM2_{C3}$. Subsequent reductive elimination yields the C(3)-isomer.^[16] The other pathway **B** involves ligation of the ruthenacycle **VI** with the in situ generated enone to form the complex $IM5_{C3}$. Subsequent migratory insertion of the enone into the $C(sp^2)$ -Ru bond generates the seven-membered intermediate $IM6_{C3}$, which following a protodemetalation, leads to the formation of the C(3)-isomer.

A third pathway **C** bifurcates into two different routes, namely **C1** and **C2**. An initial ligand exchange of the chloride/acetate with cyclopropanol (intermediate **II**) leads to the Ru-assisted ring cleaved intermediate **III**. Path **C1** involves a direct reductive elimination, assisted by ligand exchange to afford the

desired product with the regeneration of the active catalyst **I**. On the other hand, the path **C2** is characterized by a β -H elimination to form the Ru-H intermediate complex **IV**, which after successive migratory insertion (intermediate **V**) and protodemetalation yields the product molecule. To corroborate this proposed route, attempts to detect the Ru-H species or H_2 through spectroscopic means failed and this failure was further rationalized through DFT calculations (see the Supporting Information (Figures 1 and 3 and 6) for details). As evident from Scheme 7, route **C** does not involve $Cu_2(OAc)_4$ in any of the step, nevertheless induces the product formation in trace quantities (see Scheme S20B of the Supporting Information for details). This result also points towards a reduced operational probability of Path **C** into the catalytic cycle. Thus, through combined DFT calculations and experimental observations, it is evident that the pathways **A** and **B** contribute majorly in the C(3)-product formation.

For the C(4)-product formation, an oxidative transmetalation from the Cu-homoenolate **IN** and dissociation of the *p*-cym leads to the formation of the Ru/Cu bimetallic complex $IM3_{C4}$. Subsequent 1,3-alkyl migration from Ru to C center generates the intermediate $IM4_{C4}$ which is predicted to be the rate-limiting step as per the energy calculations. An intramolecular acetate assisted E2-type elimination further generates the alkene-ligated Ru complex **VII**, which after a *p*-cym ligand exchange restores the active catalyst **I**.

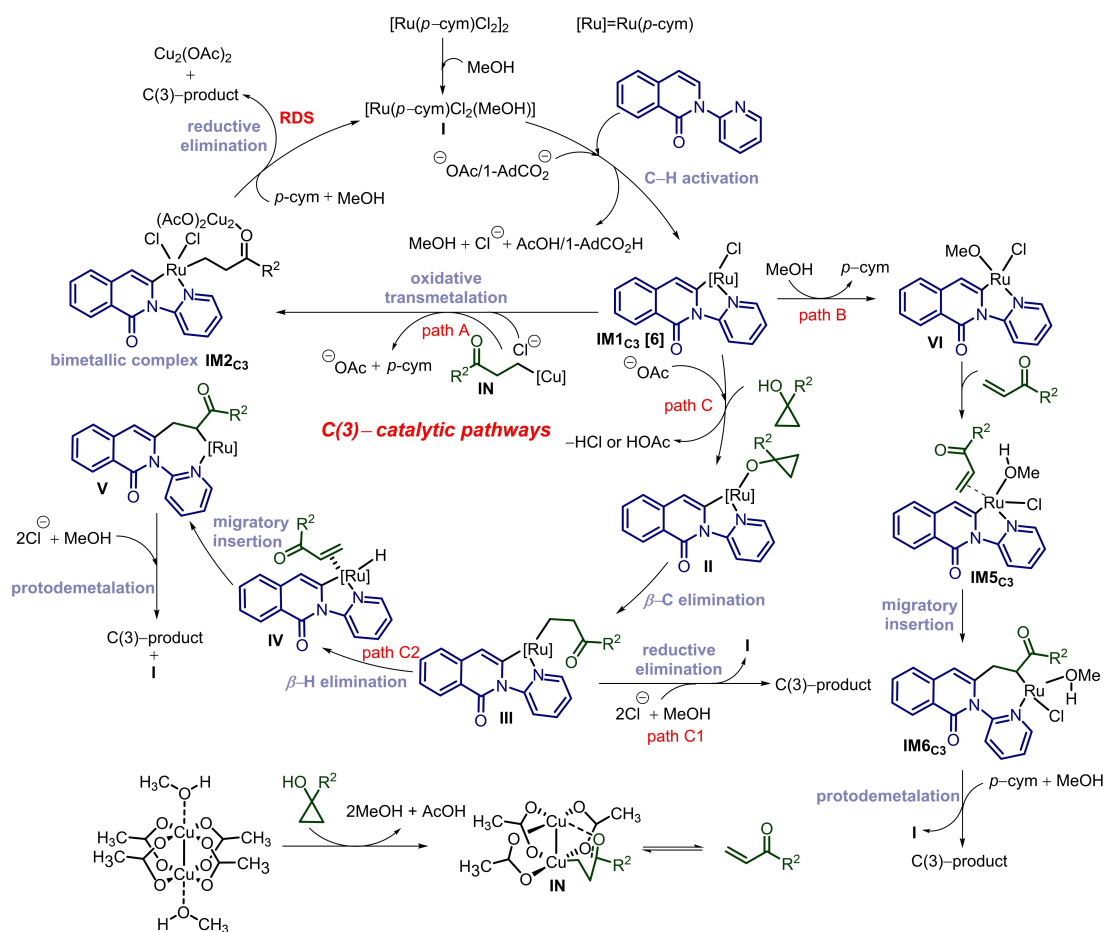
Additionally, we also investigated how substituents on the cyclopropanol substrate affect the barrier for the step involving $TS3_{C4}$, taking **2a** ($R^2 = CF_3$), **2b** ($R^2 = H$), **2g** ($R^2 = OMe$) and **2m** ($R^2 = 3,4$ -di-OMe) as representatives. As shown in Table 2, electron-withdrawing groups are predicted to lead to an increase in free energy barrier, while electron-donating groups are predicted to lead to a decrease, consistent with the regioselectivity observed experimentally. Thus, we predict from the energy calculations that the C(3)/C(4) selectivity is determined solely by the $TS3_{C4}$, which is under the control of substituent effects on cyclopropanol (see the Supporting Information for details).

Conclusions

In summary, we have developed a Ru-catalyzed, Cu-mediated ring opening of cyclopropanols and their site-selective coupling with *N*-pyridylisoquinolones in a one-pot fashion, thereby furnishing the C(3)- and C(4)-alkylated products. The strategy

Table 2. Summary of computational and experimental substituent effect studies. ΔG^\ddagger is the $TS3_{C4}(T)$ free energy activation barrier of the C(3)/C(4) selectivity determining step.

entry	R^2	C(4) ΔG^\ddagger	C(3):C(4) (experiment)
2a	CF_3	29.9	only C(3)
2b	H	28.0	3:1
2g	OMe	25.4	1:13
2m	3,4-di-OMe	24.9	only C(4)



Scheme 7. Plausible mechanistic cycle showing the C(3)- and C(4)-products formation.

remains sensitive to the electronic environment around the coupling substrates which dictates the regioselectivity of the products formed. The EWG favors the C(3)-product formation

over C(4) and *vice versa*. Hence, a diverse spectrum of β -carbonyl aryl frameworks can be accessed with the regioselectivity tuned in accordance with the electronic parameters.

Additionally, the protocol involves tandem C–C and C–H activation strategies, generating a wide array of isoquinolone derivatives in a single step, the accessibility of which are quite limited and involve multistep protocols via conventional means. Mechanistic investigations propose the simultaneous existence of singlet and triplet pathways, the energies of which dictate the product selectivity. Thus, given the ubiquity of isoquinolone skeletons in biologically and pharmaceutically active molecules, this method can improve the existing synthetic toolbox for accessing late-stage modification.

Experimental Section

General methods, procedures for the synthesis of the starting materials, experimental details for the Ru-catalyzed, Cu-mediated site-selective alkylation, further derivatization of the alkylation products and the control experiments along with mechanistic studies are described in the Supporting Information. All computational details, spectral characterization and analyses including that of SC-XRD are provided in the Supporting Information.

Deposition Numbers 2065285 (for **3b**) and 2124076 (for **4s**) contain the supplementary crystallographic data for this paper. These data are provided free of charge by the joint Cambridge Crystallographic Data Centre and Fachinformationszentrum Karlsruhe Access Structures service.

General procedure for Ru-catalyzed, Cu-mediated site-selective alkylation: In a pressure tube equipped with a magnetic stir bar, was added the corresponding 2-(pyridin-2-yl)isoquinolin-1(2H)-one (**1**, 0.1 mmol, 1.0 equiv), cyclopropanol (**2**, 0.2 mmol, 2.0 equiv) and MeOH (1 mL, HPLC grade). The reaction mixture was degassed with N₂ for 5 min followed by the addition of the [Ru(*p*-cym)Cl₂]₂ (0.04 equiv), 1-AdCO₂H (0.25 equiv), and Cu(OAc)₂·H₂O (2.1 equiv). The pressure tube was sealed under a flow of N₂, dipped into an oil bath pre-heated at 80 °C and allowed to stir for 1–3 h. The progress of the reaction was monitored by TLC. After the completion of the reaction, the crude reaction mixture was passed through a pad of Celite, washed with EtOAc (15 mL) and the solvent was removed under reduced pressure. Isolation of the product(s) was performed by silica gel flash column chromatography (230–400 mesh, eluent: Petroleum ether: EtOAc).

Supporting Information

Additional references are cited within the Supporting Information (Ref. [17–39]).

Acknowledgements

Funding from SERB-India (STR/2019/0000072) is gratefully acknowledged. NJ thanks IISERB for a Research Fellowship. We thank Dr. Pravin Kumar, IISERB, for the assistance with X-ray analysis and the CIF at IISERB for the analytical data (NMR, MS & XRD). We also thank the Director, IISERB, for funding and infrastructure facilities. WG, WYK and DJT are grateful for financial and computational support from the NSF through CHE-1856416 and the XSEDE program (CHE-030089). WYK

would like to thank the Croucher Foundation for continued financial support through a doctoral scholarship.

Conflict of Interests

The authors declare no competing financial interest.

Data Availability Statement

The data that support the findings of this study are available in the supplementary material of this article.

Keywords: C–C activation · regioisomeric ratio · Ru-catalysis · site-selective C–H alkylation · singlet and triplet states

- [1] a) A. L. Ruchelman, P. J. Houghton, N. Zhou, A. Liu, L. F. Liu, E. J. LaVoie, *J. Med. Chem.* **2005**, *48*, 792–804; b) J. Zhong, *Nat. Prod. Rep.* **2013**, *30*, 849–868.
- [2] a) S. Lee, S. Mah, S. Hong, *Org. Lett.* **2015**, *17*, 3864–3867; b) A. C. Shaikh, D. R. Shinde, N. T. Patil, *Org. Lett.* **2016**, *18*, 1056–1059; c) D. Das, R. Samanta, *Adv. Synth. Catal.* **2018**, *360*, 379–384.
- [3] a) M.-W. Chen, M. Lou, Z. Deng, Q. Ying, Y. Peng, *Asian J. Org. Chem.* **2021**, *10*, 192–195; b) H.-H. Wang, X.-D. Wang, G.-F. Yin, Y.-F. Zeng, J. Chen, Z. Wang, *ACS Catal.* **2022**, *12*, 2330–2347; c) T. Paul, S. Basak, T. Punniyamurthy, *Org. Lett.* **2022**, *24*, 6000–6005.
- [4] a) R. David, A. Orellana, *Chem. Commun.* **2013**, *49*, 5420–5422; b) H. Zhao, X. Fan, J. Yu, C. Zhu, *J. Am. Chem. Soc.* **2015**, *137*, 3490–3493; c) J. Li, Y. Zheng, M. Huang, W. Li, *Org. Lett.* **2020**, *22*, 5020–5024; d) Y. Zhou, M. Wu, Y. Liu, C. Cheng, G. Zhu, *Org. Lett.* **2020**, *22*, 7542–7546; e) B. V. Pati, A. Ghosh, K. Yadav, S. K. Banjare, S. Pandey, U. Lourderaj, P. C. Ravikumar, *Chem. Sci.* **2022**, *13*, 2692–2700; f) M. Lee, J. Heo, D. Kim, S. Chang, *J. Am. Chem. Soc.* **2022**, *144*, 3667–3675; g) X. Huang, J. Li, H. He, K. Yan, R. Lai, Y. Luo, M. Guan, Y. Wu, *Synthesis* **2022**, *54*, 779–787.
- [5] L. Souillart, N. Cramer, *Chem. Rev.* **2015**, *115*, 9410–9464.
- [6] T. A. Shah, P. B. De, S. Pradhan, S. Banerjee, T. Punniyamurthy, *Chem. Asian J.* **2019**, *14*, 4520–4533.
- [7] a) X. Zhou, S. Yu, L. Kong, X. Li, *ACS Catal.* **2016**, *6*, 647–651; b) X. Zhou, S. Yu, Z. Qi, L. Kong, X. Li, *J. Org. Chem.* **2016**, *81*, 4869–4875; c) J. Liu, Z. Yang, J. Jiang, Q. Zeng, L. Zheng, Z.-Q. Liu, *Org. Lett.* **2021**, *23*, 5927–5931; d) K. Ramachandran, P. Anbarasan, *Chem. Commun.* **2022**, *58*, 10536–10539; e) K. Ramachandran, P. Anbarasan, *Org. Lett.* **2022**, *24*, 6745–6749.
- [8] a) V. K. Tiwari, G. G. Pawar, H. K. Jena, M. Kapur, *Chem. Commun.* **2014**, *50*, 7322–7325; b) V. K. Tiwari, N. Kamal, M. Kapur, *Org. Lett.* **2017**, *19*, 262–265; c) R. Das, N. K. Khot, A. S. Deshpande, M. Kapur, *Synthesis*. **2019**, *51*, 2515–2522; d) N. Jha, R. P. Singh, P. Saxena, M. Kapur, *Org. Lett.* **2021**, *23*, 8694–8698.
- [9] For a recent review on HFIP, see: H. F. Motiwala, A. M. Armaly, J. G. Cacioppo, T. C. Coombs, K. R. K. Koehn, V. M. Norwood IV, J. Aube, *Chem. Rev.* **2022**, *122*, 12544–12747.
- [10] a) Z. Ye, K. E. Gettys, X. Shen, M. Dai, *Org. Lett.* **2015**, *17*, 6074–6077; b) Z. Ye, X. Cai, J. Li, M. Dai, *ACS Catal.* **2018**, *8*, 5907–5914; c) W. Liang, X. Cai, M. Dai, *Chem. Sci.* **2021**, *12*, 1311–1316.
- [11] A. E. Shilov, G. B. Sul'pin, *Chem. Rev.* **1997**, *97*, 2879–2932.
- [12] E. A. Trifonova, N. M. Ankudinov, M. V. Kozlov, M. Y. Sharipov, Y. V. Nelyubina, D. S. Perekalin, *Chem. Eur. J.* **2018**, *24*, 16570–16575.
- [13] a) C. Adamo, V. Barone, *J. Chem. Phys.* **1999**, *110*, 6158–6172; b) F. Weigend, R. Ahlrichs, *Phys. Chem. Chem. Phys.* **2005**, *7*, 3297–3305; c) A. V. Marenich, C. J. Cramer, D. G. Truhlar, *J. Phys. Chem. B.* **2009**, *113*, 6378–6396; d) S. Grimme, S. Ehrlich, L. Goerigk, *J. Comput. Chem.* **2011**, *32*, 1456–1465; e) E. Caldeweyher, S. Ehlert, A. Hansen, H. Neugebauer, S. Spicher, C. Bannwarth, S. Grimme, *J. Chem. Phys.* **2019**, *150*, 154122.
- [14] P. Pracht, F. Bohle, S. Grimme, *Phys. Chem. Chem. Phys.* **2020**, *22*, 7169–7192.
- [15] T. P. Gomba, N. Jiang, H. S. La Pierre, *Dalton Trans.* **2019**, *48*, 16869–16872.

- [16] J. Kim, K. Shin, S. Jin, D. Kim, S. Chang, *J. Am. Chem. Soc.* **2019**, *141*, 4137–4146.
- [17] a) L. Cardinale, M. Neumeier, M. Majek, A. J. von Wangelin, *Org. Lett.* **2020**, *22*, 7219–7224; b) X.-P. He, Y.-J. Shu, J.-J. Dai, W.-M. Zhang, Y.-S. Feng, H.-J. Xu, *Org. Biomol. Chem.* **2015**, *13*, 7159–7163; c) K. Jia, F. Zhang, H. Huang, Y. Chen, *J. Am. Chem. Soc.* **2016**, *138*, 1514–1517; d) Q. Liu, Q. Wang, G. Xie, Z. Fang, S. Ding, X. Wang, *Eur. J. Org. Chem.* **2020**, *2020*, 2600–2604; e) S. Wang, E. Miao, H. Wang, B. Song, W. Huang, W. Yang, *Chem. Commun.* **2021**, *57*, 5929–5932; f) S. R. Shirsath, S. M. Chandgude, M. Muthukrishnan, *Chem. Commun.* **2021**, *57*, 13582–13585; g) A. Ilangoan, S. Saravanakumar, S. Malayappasamy, *Org. Lett.* **2013**, *15*, 4968–4971; h) Y. A. Konik, G. Z. Elek, S. Kaabel, I. Jarving, M. Loop, D. G. Kananovich, *Org. Biomol. Chem.* **2017**, *15*, 8334–8340; i) Y.-F. Wang, S. Chiba, *J. Am. Chem. Soc.* **2009**, *131*, 12570–12572; j) S. Ren, C. Feng, T.-P. Loh, *Org. Biomol. Chem.* **2015**, *13*, 5105–5109.
- [18] X. Y. Dong, Y. F. Zhang, C. L. Ma, Q. S. Gu, F. L. Wang, Z. L. Li, S. P. Jiang, X. Y. Liu, *Nat. Chem.* **2019**, *11*, 1158–1166.
- [19] M. Zaheer, M. Zia-ur-Rehman, R. Munir, N. Jamil, S. Ishtiaq, R. S. Z. Saleem, M. R. J. Elsegood, *ACS Omega* **2021**, *6*, 31348–31357.
- [20] A. Cook, S. Prakash, Y.-L. Zheng, S. G. Newman, *J. Am. Chem. Soc.* **2020**, *142*, 8109–8115.
- [21] J. Liu, E. Xu, J. Jiang, Z. Huang, L. Zheng, Z.-Q. Liu, *Chem. Commun.* **2020**, *56*, 2202–2205.
- [22] a) Y. Jin, Y. Makida, T. Uchida, R. Kuwano, *J. Org. Chem.* **2018**, *83*, 3829–3839; b) A. Jakab, Z. Dalicsek, T. Holczbauer, T. Hamza, I. Pápai, Z. Finta, G. Timári, T. Soós, *Eur. J. Org. Chem.* **2015**, *2015*, 60–66; c) A. R. Choudhury, S. Mukherjee, *Chem. Sci.* **2016**, *7*, 6940–6945; d) V. D. Cao, D. G. Jo, H. Kim, C. Kim, S. Yun, S. Joung, *Synthesis* **2021**, *53*, 754–764.
- [23] a) Y. Cui, D. Bai, B. Liu, J. Chang, X. Li, *Chem. Commun.* **2020**, *56*, 15631–15634.
- [24] P. Peng, J. Wang, H. Jiang, H. Liu, *Org. Lett.* **2016**, *18*, 5376–5379.
- [25] M. Guimond, S. I. Gorelsky, K. Fagnou, *J. Am. Chem. Soc.* **2011**, *133*, 6449–6457.
- [26] S. Lin, Z. Zhang, J. Chen, Y. Luo, Y. Xia, *Org. Lett.* **2022**, *24*, 3302–3306.
- [27] N. J. Webb, S. P. Marsden, S. A. Raw, *Org. Lett.* **2014**, *16*, 4718–4721.
- [28] B. Yu, S. Mohamed, J. Ardisson, M.-I. Lannou, G. Sorin, *Chem. Commun.* **2022**, *58*, 1374–1377.
- [29] Y.-Q. Zhu, Y.-X. Niu, L.-W. Hui, J.-L. He, K. Zhu, *Adv. Synth. Catal.* **2019**, *361*, 2897–2903.
- [30] Y.-Q. Zhu, L.-W. Hui, S.-B. Zhang, *Adv. Synth. Catal.* **2021**, *363*, 2170–2176.
- [31] M. J. Frisch, G. W. Trucks, H. B. Schlegel, G. E. Scuseria, M. Robb, J. R. Cheeseman, G. Scalmani, V. Barone, G. A. Petersson, H. Nakatsuji, X. Li, M. Caricato, A. V. Marenich, J. Bloino, B. G. Janesko, R. Gomperts, B. Mennucci, H. P. Hratchian, J. V. Ortiz, A. F. Izmaylov, J. L. Sonnenberg, D. Williams-Young, F. Ding, F. Lipparini, F. Egidi, J. Goings, B. Peng, A. Petrone, T. Henderson, D. Ranasinghe, V. G. Zakrzewski, J. Gao, N. Rega, G. Zheng, W. Liang, M. Hada, M. Ehara, K. Toyota, R. Fukuda, J. Hasegawa, M. Ishida, T. Nakajima, Y. Honda, O. Kitao, H. Nakai, T. Vreven, K. Throssell, J. A. Montgomery, Jr., J. E. Peralta, F. Ogliaro, M. J. Bearpark, J. J. Heyd, E. N. Brothers, K. N. Kudin, V. N. Staroverov, T. A. Keith, R. Kobayashi, J. Normand, K. Raghavachari, A. P. Rendell, J. C. Burant, S. S. Iyengar, J. Tomasi, M. Cossi, J. M. Millam, M. Klene, C. Adamo, R. Cammi, J. W. Ochterski, R. L. Martin, K. Morokuma, O. Farkas, J. B. Foresman, D. J. Fox, Gaussian 16, Revision C.01, Gaussian, Inc., WallingfordCT, 2016.
- [32] F. Neese, *WIREs Comput. Mol. Sci.* **2022**, *12*, e1606.
- [33] F. Neese, F. Wennmohs, A. Hansen, U. Becker, *Chem. Phys.* **2009**, *356*, 98–109.
- [34] F. Weigend, *Phys. Chem. Chem. Phys.* **2006**, *8*, 1057–1065.
- [35] a) L. R. Maurer, M. Bursch, S. Grimme, A. Hansen, *J. Chem. Theory Comput.* **2021**, *17*, 6134–6151; b) S. Dohm, A. Hansen, M. Steinmetz, S. Grimme, M. P. Checinski, *J. Chem. Theory Comput.* **2018**, *14*, 2596–2608.
- [36] K. Fukui, *Acc. Chem. Res.* **1981**, *14*, 363–368.
- [37] a) S. Grimme, *Chem. Eur. J.* **2012**, *18*, 9955–9964; b) G. Luchini, V. Alegre-Requena, I. Funes-Ardoiz, R. S. Paton, *F1000Research* **2020**, *9*, 291.
- [38] M. Álvarez-Moreno, C. De Graaf, N. Lopez, F. Maseras, J. M. Poblet, C. Bo, *J. Chem. Inf. Model.* **2015**, *55*, 95–103.
- [39] a) I. Funes-Ardoiz, F. Maseras, *Angew. Chem. Int. Ed.* **2016**, *128*, 2814–2817; b) A. W. Jones, C. K. Rank, Y. Becker, C. Malchau, I. Funes-Ardoiz, *Chem. Eur. J.* **2018**, *24*, 15178–15184.

Manuscript received: May 17, 2023

Accepted manuscript online: July 5, 2023

Version of record online: September 1, 2023